

Scaled Quantum Chemical Calculations and FTIR, FT-Raman Spectra, NBO, Thermodynamical behavior, HOMO-LUMO and Electronic Structure Calculations on 4-(Dimethylamine) Benzophenone

M. Karnan^{1,*}, V. Balachandran², M. Murugan³ and M.K. Murali⁴

¹Department of Physics, Srimad Andavan Arts and Science College, Tiruchirappalli-5, India.

²Department of Physics, A. A. Government Arts College, Musiri 621211, India.

³Department of Physics, Government Arts College, Tiruchirappalli, 620022, India.

⁴Department of Physics, J.J College of Arts and Science, Pudukotti, 622404, India.

ARTICLE INFO

Article history:

Received: 27 December 2015;

Received in revised form:

28 January 2016;

Accepted: 3 February 2016;

Keywords

4-(Dimethylamine)
Benzophenone,
Vibrational Spectra,
HOMO-LUMO,
NBO,
MEP Surface.

ABSTRACT

In this work, experimental and theoretical study on the molecular structure, scaled quantum chemical calculations of energies and vibrational wavenumbers of 4-(dimethylamine) benzophenone (4DMBP) is presented. The vibrational frequencies of the title compound were obtained theoretically by DFT/B3LYP calculations employing the standard 6-311+G(d,p) and 6-311++G(d,p) basis sets for optimized geometry and were compared with Fourier transform infrared spectrum (FTIR) in the region of 4000 – 400 cm⁻¹ and Fourier transform Raman spectrum in the region of 4000 – 100 cm⁻¹. Complete vibrational assignments, analysis and correlation of the fundamental modes for the title compound were carried out. The vibrational harmonic frequencies were scaled using scale factor, yielding a good agreement between the experimentally recorded and the theoretically calculated values. The study is extended to calculate the HOMO-LUMO energy gap, NBO, mapped molecular electrostatic potential (MEP) surfaces, polarizability, Mulliken charges and thermodynamic properties of the title compound.

© 2016 Elixir all rights reserved.

Introduction

Benzophenone, an aromatic ketones (diphenyl ketone), is an important compound in organic photochemistry and perfumery as well as in organic synthesis. It is a white crystalline substance with rose-like odor; insoluble in water; melting point 49°C; boiling point 305° – 306°C. Benzophenone is used as a constituent of synthetic perfumes and as a starting material for the manufacture of dyes, pesticides and drugs (especially anxiolytic and hypnotic drugs). Benzophenone is used as a photoinitiator of UV-curing applications in inks, adhesive and coatings, optical fiber as well as in printed circuit boards. Photoinitiators are compounds that break down into free radicals upon exposure to ultraviolet radiation. Photoinitiators undergo a unimolecular bond cleavage upon irradiation to yield free radicals (benzoin esters; benzil ketals; alpha-dialkoxy acetophenones; alpha-hydroxy alkylphenones; alpha-amino alkylphosphine; acylphosphine oxides). Another type of photoinitiators undergo a bimolecular reaction where the excited state of the photoinitiator interacts with a second molecule (a coinitiator) to generate free radicals (benzophenones, amines; thioxanthenes, titanocenes). Ultraviolet radiation has more energy than visible light, and thus degrade the physical properties such as the appearance of organic substances and plastics. Benzophenones can act as optical filters or deactivate substrate molecules that have been excited by light for the protection polymers and organic substances. They, cosmetic grades, are used as sunscreen agents to reduce skin damage by blocking UV-A, B.

The procedure whereby vibrational spectra are classified by assigning normal mode quantum numbers to the vibrational states has proven immensely useful in molecular spectroscopy. Large numbers of levels are observed for which the normal mode assignments are well defined and are very successful in organizing and interpreting the spectral data. The vibrational analysis of benzophenone and its derivatives would be helpful for understanding the various types of bonding and normal modes of vibration. Current computational methods can provide a useful description of the vibrational spectra of the ground and lowest electronically excited states of organic molecules. The vibrational spectra of benzophenone, mono-substituted benzophenones and disubstituted benzophenones have been studied extensively, for example: The spectral studies on the vibrational frequencies of mono and dihalogenated benzophenones were reported by a few authors [1–3]. Giorgianni *et al.* have reported different vibrational frequencies of h₁₀ and d₁₀-benzophenones and a series of symmetrically and unsymmetrically substituted 4, 4'-dihalogeno benzophenones [1]. Recently, crystal structure, molecular structure and vibrational spectra of benzophenone and α -4-methylbenzophenone by density functional theory calculations have been carried out by Sasiadek *et al.* [4, 5] and their results were verified by density functional method using 6-311+G(d,p) and 6-311++G(d,p) basis sets.

Literature survey reveals that so far there is no complete theoretical study for the title compounds 4DMBP. In this work, we mainly focused on the detailed spectral assignments and vibrational thermodynamic properties based on the

experimental Fourier transform infrared (FT-IR) and Fourier transform Raman (FT-Raman) spectra as well as DFT/B3LYP calculations for 4DMBP. The redistribution of electron density (ED) in various bonding, antibonding orbitals and E(2) energies have been calculated by natural bond orbital (NBO) analysis to give clear evidence of stabilization originating from the hyper conjugation of various intra-molecular interactions. The study of HOMO, LUMO analysis has been used to elucidate information regarding charge transfer within the molecule. Finally, electronic absorption properties were explained and illustrated from the frontier molecular orbitals. Here, the calculated results have been reported in the text. The experimental and theoretical results supported each other, and the calculations are valuable for providing insight into the vibrational spectra and molecular properties.

2 Experimental Details

The sample 4DMBP was purchased from Lancaster Chemical Company, U.K with a stated purity of greater than 97%, and it was used as such for the spectral measurements. The room temperature Fourier transform infrared spectra of 4DMBP was recorded in the region 4000–400 cm^{-1} at a resolution of $\pm 1 \text{ cm}^{-1}$, using BRUKER IFS-66V Fourier transform spectrometer, equipped with an MCT detector, a KBr beam splitter and global source. The FT-Raman spectrum was recorded on the same instrument with FRA-106 Raman accessories in the region 3500–100 cm^{-1} . Nd:YAG laser operating at 200 mw power with 1064 nm excitation was used as source.

3 Computational Details

The molecular geometry optimization and vibrational frequency calculations were carried out for 4DMBP, with GAUSSIAN 09W software package [6] the density functional method used is B3LYP i.e. Becke's three-parameter hybrid functional with the Lee-Yang-Parr correlation functional method [7, 8] combined with standard 6-311+G(d,p) and 6-311++G(d,p) basis sets. Scaling of the force field was performed according to the SQM procedure [9, 10] using selective scaling in the natural internal coordinate representation [11]. Transformation of the force field and subsequent normal coordinate analysis including the least square refinement of the scale factors, calculation of the potential energy distribution [PED] and the prediction of FTIR and FT Raman intensities were done on a PC with the MOLVIB Program (version 7.0-G77) written by Sundius [12]. For the plots of simulated Raman spectra, pure Lorentzian band shapes were used with a bandwidth of 10 cm^{-1} . Finally the calculated normal mode vibrational frequencies provide atomic charges and thermodynamic properties also through the principle of statistical mechanics.

4 Prediction of Raman Intensities

The Raman activities (S_i) calculated with the GAUSSIAN 09 program and adjusted during the scaling procedure with MOLVIB were subsequently converted to relative Raman intensities (I_i) using the following relationship derived from the theory of Raman scattering [13, 14].

$$I_{Ra} = \frac{f(\nu_0 - \nu_i)^4 S_{Ra}}{\nu_i \left[1 - \exp\left(-\frac{hc\nu_i}{kT}\right) \right]}$$

where

ν_0 is the exciting frequency (in cm^{-1})

ν_i is the vibrating wave number of the i^{th} normal mode

h , c and k are the fundamental constants and f is a normalization factor for all peak intensities.

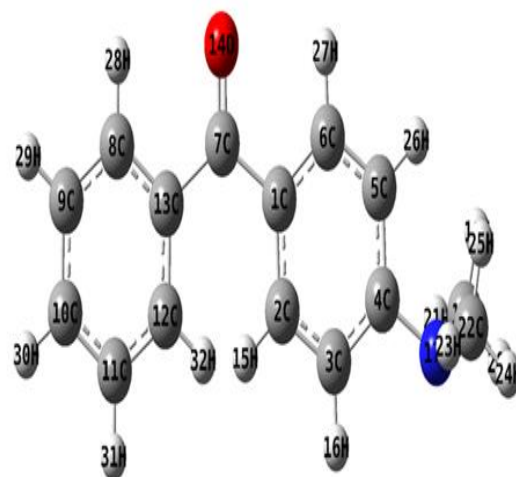


Fig 1. Geometrical structure of 4-(dimethylamino)benzophenone

5 Results and Discussion

Optimized geometry

The first task for the computational work is to determine the optimized geometries of the studied molecule. The geometry of the molecule under investigation is considered by possessing C1 point group symmetry. The 4DMBP is an asymmetric top. The comparative optimized structural parameters such as bond lengths, bond angles and dihedral angles are presented in Table 1 in accordance with atom numbering scheme shown in Fig. 1. The optimized geometry calculation is performed using B3LYP/6-311+G(d,p) and 6-311++G(d,p) basis sets of theoretical approximation for 4DMBP compound. Since the exact crystal structure of the 4DMBP compound is not available till now, the optimized structure can be only compared with other similar system benzophenone [15] for which the crystal structure has been solved. The calculated C–C bond lengths of the phenyl ring vary from 1.38 to 1.50 Å. The C5–C6 and C7–C13 bond lengths are slightly larger than other C–C bonds, indicating conjugation of carbonyl group with the two phenyl ring systems. However, the phenyl ring (Ph1) appears to be a little distorted from its regular hexagonal symmetry. DFT calculation indicates increase in the angles C2–C1–C7 (4.40°) and C2–C3–C4 (1.00°) and reduction in the angles C3–C4–C5 (2.75°) and C6–C1–C7 (1.96°) from 120.0°, associated with the charge transfer interactions on substitution with CH₃ group atom. The deviations of C1–C7–O14 (120.44°), C13–C7–O14 (118.80°) bond angles are due to the electronic coupling between the carbonyl oxygen lone pair electrons and the phenyl ring π -system. The structure of the molecule deviates significantly from planarity because the two phenyl rings are rotated around the C–C = O–C axes. The phenyl rings are twisted relative to the planar group C–C=O–C to give a C2–C1–C7–O14 and C6–C1–C7–O14 dihedral angle of 156.65° and –18.85°.

6 Vibrational Assignments

In order to obtain the spectroscopic signature of the selected compound, we performed a frequency calculation analysis.

Table 1. Optimized structural parameters of 4-(dimethylamine) benzophenone utilizing DFT-B3LYP/6-311+G (d,p) and 6-311++G(d,p) density functional calculation

Bond length	Value(Å)		Bond angle	Value(°)		Dihedral angle	Value(°)	
	6-311+G(d,p)	6-311++G(d,p)		6-311+G(d,p)	6-311++G(d,p)		6-311+G(d,p)	6-311++G(d,p)
C1-C2	1.407	1.409	C2-C1-C6	117.306	117.464	C6-C1-C2-C3	-1.078	-1.048
C1-C6	1.409	1.411	C2-C1-C7	124.408	124.078	C6-C1-C2-H15	176.809	176.980
C1-C7	1.489	1.480	C6-C1-C7	118.142	118.341	C7-C1-C2-C3	-176.623	-177.058
C2-C3	1.391	1.391	C1-C2-C3	121.637	121.532	C7-C1-C2-H15	1.264	0.970
C2-H15	1.091	1.084	C1-C2-H15	119.981	119.841	C2-C1-C6-C5	2.040	1.833
C3-C4	1.419	1.420	C3-C2-H15	118.349	118.598	C2-C1-C6-H27	-177.893	-178.176
C3-H16	1.089	1.082	C2-C3-C4	121.000	120.905	C7-C1-C6-C5	177.872	178.078
C4-C5	1.422	1.422	C2-C3-H16	118.569	118.781	C7-C1-C6-H27	-2.061	-1.930
C4-N17	1.379	1.385	C4-C3-H16	120.430	120.311	C2-C1-C7-C13	-23.257	-23.408
C5-C6	1.386	1.386	C3-C4-C5	117.257	117.518	C2-C1-C7-O14	156.657	156.558
C5-H26	1.089	1.082	C3-C4-N17	121.426	121.288	C6-C1-C7-C13	161.232	160.615
C6-H27	1.091	1.085	C5-C4-N17	121.316	121.193	C6-C1-C7-O14	-18.854	-19.419
C7-C13	1.508	1.498	C4-C5-C6	120.876	120.782	C1-C2-C3-C4	-0.857	-0.444
C7-O14	1.228	1.258	C4-C5-H26	120.383	120.267	C1-C2-C3-H16	178.683	178.922
C8-C9	1.394	1.395	C6-C5-H26	118.740	118.950	H15-C2-C3-C4	-178.777	-178.497
C8-C13	1.406	1.408	C1-C6-C5	121.881	121.771	H15-C2-C3-H16	0.762	0.869
C8-H28	1.091	1.084	C1-C6-H27	117.977	118.012	C2-C3-C4-C5	1.828	1.175
C9-C10	1.400	1.402	C5-C6-H27	120.142	120.218	C2-C3-C4-N17	-178.420	-179.161
C9-H29	1.093	1.085	C1-C7-C13	120.752	121.229	H16-C3-C4-C5	-177.703	-178.182
C10-C11	1.397	1.399	C1-C7-O14	120.443	120.141	H16-C3-C4-N17	2.050	1.483
C10-H30	1.093	1.086	C13-C7-O14	118.805	118.630	C3-C4-C5-C6	-0.885	-0.406
C11-C12	1.398	1.399	C9-C8-C13	120.650	120.621	C3-C4-C5-H26	178.718	179.311
C11-H31	1.093	1.086	C9-C8-H28	121.074	121.054	N17-C4-C5-C6	179.363	179.929
C12-C13	1.405	1.407	C13-C8-H28	118.275	118.324	N17-C4-C5-H26	-1.035	-0.354
C12-H32	1.091	1.084	C8-C9-C10	120.038	120.046	C3-C4-N17-C18	-175.070	-0.087
N17-C18	1.452	1.463	C8-C9-H29	119.921	119.911	C3-C4-N17-C22	-4.176	-179.021
N17-C22	1.452	1.464	C10-C9-H29	120.039	120.042	C5-C4-N17-C18	4.673	179.566
C18-H19	1.107	1.098	C9-C10-C11	119.802	119.824	C5-C4-N17-C22	175.566	0.632
C18-H20	1.097	1.091	C9-C10-H30	120.123	120.104	C4-C5-C6-C1	-1.067	-1.121
C18-H21	1.104	1.099	C11-C10-H30	120.073	120.069	C4-C5-C6-H27	178.864	178.888
C22-H23	1.104	1.099	C10-C11-C12	120.164	120.164	H26-C5-C6-C1	179.324	179.159
C22-H24	1.097	1.091	C10-C11-H31	120.083	120.074	H26-C5-C6-H27	-0.745	-0.833
C22-H25	1.107	1.098	C12-C11-H31	119.753	119.761	C1-C7-C13-C8	149.734	150.695

The main focus on the present investigation is the proper assignment of the experimental frequencies to the various vibrational modes of 4DMBP in corporation with the scaled down calculated harmonic vibrational frequencies at B3LYP level using 6-311++G (d,p) basis set. The molecule belongs to the C₁ point group. The atomic displacements corresponding to the different normal modes are identified using Gauss View program package [16]. The comparative IR and Raman spectra of experimental and simulated (B3LYP) are given in Figs 2 and 3 respectively. The observed and calculated frequencies along with their relative intensities, probable assignments and potential energy distribution (PED) of 4DMBP are summarized in Table 2.

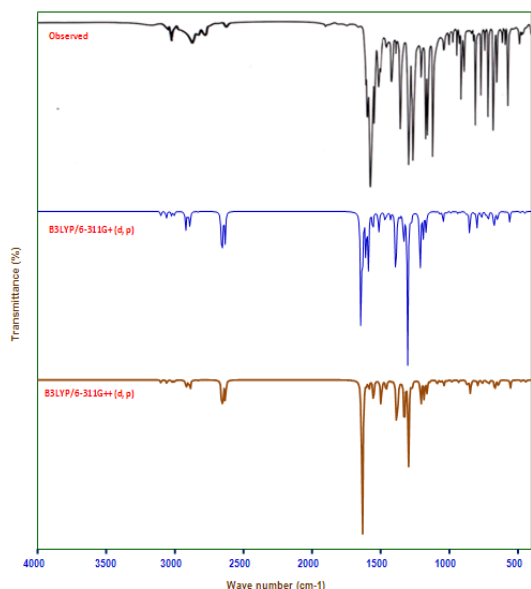


Fig 2. Observed FT-IR and simulated spectrum of 4-(dimethylamino) benzophenone (a) Observed (b) B3LYP/6-311+G(d,p) (c) B3LYP/6-311++G(d,p)

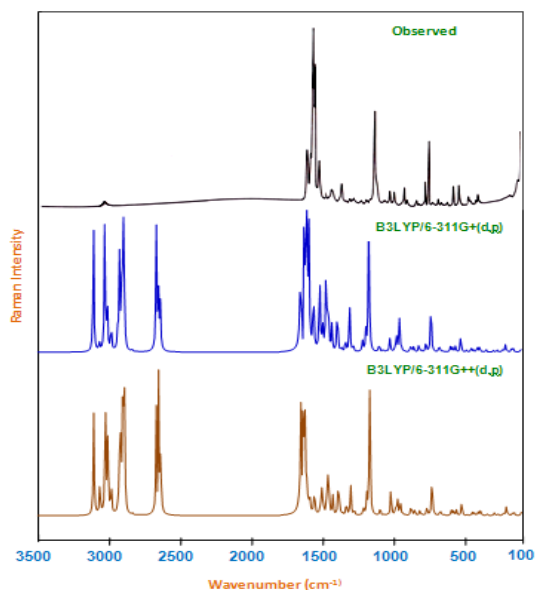


Fig 3. Observed FT-Raman and simulated spectrum of 4-(dimethylamino) benzophenone (a) Observed (b) B3LYP/6-311+G(d,p) (c) B3LYP/6-311++G(d,p)

A dual scaling factor gives better agreement between the calculated and observed wavenumbers, in comparison to uniform scaling factor. In view of these forgoing discussion dual scaling method in which the scaling factors are 0.9927 and 0.9659 for the fingerprint (below 1800 cm⁻¹) and stretching (above 1800 cm⁻¹) regions,

respectively were used in this study to offset the systematic error caused by neglecting harmonicity and electron density [17]. The scaled calculated frequencies minimize the root-mean square difference between calculated and experimental frequencies for bands with definite identifications.

CH₃ Vibrations

Vibrational spectral studies on esters have shown that asymmetric and symmetric methyl stretching band can be observed around 2960 and 2846 cm⁻¹, respectively [18-21]. For the assignments of CH₃ group wavenumbers one can expect nine fundamentals can be associated with each CH₃ group, namely CH₃ ss (symmetric stretching), CH₃ as (asymmetric stretching), CH₃ ips (in-plane stretching), CH₃ sb (symmetric bending), CH₃ ipb (in-plane bending), CH₃ opb (out-of-plane bending), CH₃ ipr (in-plane rocking), CH₃ opr (out-of-plane rocking) and τCH₃ (twisting) modes. For the methoxy group compounds [22], the asymmetric stretching mode appears in the range 2825–2870 cm⁻¹, lower in magnitude compared to its value in CH₃ compounds (2860–2935 cm⁻¹) whereas the asymmetric stretching modes for the compounds lie in the same region 2925–2985 cm⁻¹. The weak bands observed at 2875 and 2813 cm⁻¹ in the FT-IR spectrum could be attributed to CH₃ asymmetric stretching vibration.

The theoretically computed values of 2878, 2818, 2659, 2655, 2649 and 2630 cm⁻¹ by B3LYP/6-311++G (d,p) method show good agreement with experimental results for asymmetric and symmetric stretching vibrations of CH₃ group, respectively. The bending vibrations of CH₃ group is usually observed at around 1450 cm⁻¹ for methyl substituted benzenes [23]. As expected, medium intensity band appeared at 1436 cm⁻¹ in FT-IR spectrum is due to CH₃ ipb bending vibration. The band in the FT-Raman spectrum appears at 1370 cm⁻¹ for CH₃ opb vibration. The calculated CH₃ bending vibration occurs at 1372 cm⁻¹. The theoretically calculated value also coincides very well with the experimental values.

The medium intensity band observed at 1028 cm⁻¹ in the FT-IR spectrum could be assigned to CH₃ in-plane rocking vibration. The computed value by B3LYP/6-311++G (d,p) method at 1028 cm⁻¹ shows excellent agreement with experimental data. The CH₃ (methyl twisting mode) vibrations were assigned within the characteristic region and reported in Table 2. The torsional modes of methoxy group, which are strongly coupled with some other vibrations, are observed which is in agreement with the calculated results also.

C–H vibrations

The existence of one or more aromatic rings in a structure is normally readily determined from the C–H and C–C ring related vibrations. The C–H stretching occurs above 3000 cm⁻¹ and is typically exhibited as a multiplicity of weak to moderate bands, compared with the aliphatic C–H stretch [24]. These vibrations are not found to be affected due to the nature and position of the substituents. In our present work, the C–H stretching vibration is observed in FT-IR spectrum at 3042 and 2917cm⁻¹ and in FT-Raman spectrum at 3087 cm⁻¹. The similar vibration is calculated in the range 3092 – 2894 cm⁻¹ by B3LYP/6-311++G (d,p) method and it shows good correlation with the experimental data. As indicated by the PED, these modes involve more than 90% of contribution suggesting that they are pure stretching modes. All the aromatic C–H stretching bands are found to be weak and this is due to the decrease of dipole moment caused by the reduction of negative charge on the carbon atom.

Table 2. Experimental and Calculated DFT-B3LYP/6-311+G(d,p) and 6-311++G(d,p) levels of vibrational frequencies (cm⁻¹), IR intensity (kmmol⁻¹) and Raman activity (Å⁴ amu⁻¹) of 4-(dimethylamine) benzophenone

No	Spe.	Observed Frequencies (cm ⁻¹)		Calculated frequencies (cm ⁻¹)				IR Intensity (kmmol ⁻¹)		Raman intensity (kmmol ⁻¹)		Vibrational assignments /PED (≥ 10%)
		IR	Raman	DFT-B3LYP		6-311++G(d,p)		6-311+G(d,p)	6-311++G(d,p)	6-311+G(d,p)	6-311++G(d,p)	
				6-311+G(d,p)	6-311++G(d,p)	6-311+G(d,p)	6-311++G(d,p)					
1	A		3087	3244	3100	3222	3092	9.854	11.400	7.133	11.861	vCH(99)
2	A	3042		3242	3057	3221	3041	13.623	21.031	2.146	0.862	vCH(98)
3	A			3234	3029	3209	3019	8.557	11.527	7.883	12.094	vCH(98)
4	A			3228	3006	3204	3001	7.847	12.409	5.809	4.491	vCH(97)
5	A			3223	2983	3202	2978	0.544	1.062	1.815	2.365	vCH(98)
6	A	2917		3218	2929	3196	2920	2.473	2.621	0.729	1.589	vCH(98)
7	A			3215	2919	3193	2915	34.594	46.554	6.990	8.444	vCH(99)
8	A			3203	2899	3181	2902	11.141	14.014	6.283	8.065	vCH(98)
9	A			3192	2898	3170	2894	0.284	0.106	2.136	2.876	vCH(99)
10	A	2875		3165	2889	3142	2878	35.556	44.468	9.382	12.054	CH ₃ ass(98)
11	A	2813		3152	2823	3130	2818	1.899	2.220	0.120	0.221	CH ₃ ass(97)
12	A			3070	2662	3049	2659	48.154	64.810	4.315	4.196	CH ₃ ass(97)
13	A			3066	2658	3047	2655	22.970	17.703	5.023	6.993	CH ₃ ass(97)
14	A			3022	2652	2994	2649	93.684	76.280	14.275	17.530	CH ₃ ss(93)
15	A			3014	2633	2986	2630	80.583	84.285	4.421	4.838	CH ₃ ss(96)
16	A		1636	1674	1645	1656	1639	142.184	266.840	47.055	48.657	vCO(88)
17	A	1628		1660	1637	1656	1631	502.082	67.266	100.000	27.684	vCC(69), βCH(17)
18	A	1606	1609	1649	1630	1643	1610	25.155	98.534	56.974	91.926	vCC(64), βCH(21)
19	A		1596	1626	1608	1619	1602	12.463	128.046	3.998	100.000	vCC(63), βH(18)
20	A	1574	1576	1592	1584	1591	1576	31.126	151.209	3.248	39.946	vCC(71), βCH(22)
21	A	1543	1544	1585	1551	1559	1546	95.216	55.418	5.991	21.126	vCC(66), βCH(17)
22	A			1571	1508	1516	1500	5.678	61.876	3.004	27.534	vCC(81), βCH(16)
23	A		1482	1560	1489	1504	1486	99.095	4.015	7.710	1.862	βCH(60), vCC(16)
24	A	1468		1549	1466	1493	1464	5.085	0.133	0.865	8.358	βCH(60), vCC(21)
25	A		1454	1536	1458	1472	1456	0.383	14.085	1.942	19.827	βCH(69), vCC(11)
26	A	1436		1526	1454	1471	1440	18.655	3.520	2.372	4.139	CH ₃ ipb(38), vCC(12)
27	A			1526	1446	1463	1438	18.529	4.501	3.659	3.687	CH ₃ ipb(67), vCC(17)
28	A			1503	1423	1440	1391	9.836	9.804	9.142	8.255	CH ₃ opb(66), vCC(14)
29	A	1372	1370	1496	1392	1412	1370	0.776	4.305	2.225	14.901	CH ₃ opb(51), vCC(14)
30	A	1362		1484	1383	1401	1360	3.520	18.108	5.374	10.240	vCC(49), CH ₃ opb(16)
31	A	1319	1315	1408	1373	1390	1317	208.237	215.879	10.381	18.018	vCC(46), CH ₃ opb(15)
32	A		1305	1395	1361	1378	1305	59.863	13.963	2.452	0.675	CH ₃ sb(76)
33	A	1287		1387	1293	1360	1285	3.177	11.747	0.595	1.585	CH ₃ sb(79)
34	A			1380	1267	1334	1264	177.675	57.608	3.327	3.239	βCH(43), vCC(13)
35	A			1366	1243	1330	1240	31.314	36.632	0.726	1.957	βCH(67), vCC(22)
36	A		1239	1335	1241	1303	1238	315.841	411.233	9.803	20.266	βCH(42), vCC(13)
37	A	1223		1289	1230	1276	1227	31.171	29.520	1.819	3.271	vCC(71), βCH(13)
38	A	1202	1207	1256	1206	1212	1203	99.066	174.259	2.578	6.148	vCC(68), βCH(23)
39	A			1235	1183	1189	1181	14.144	63.128	5.375	2.104	βCH(69), vCC(15)
40	A	1180		1223	1182	1188	1179	52.689	0.136	1.453	8.397	βCH(72), vCC(14)
41	A			1222	1165	1171	1162	5.745	13.754	9.562	8.326	βCH(71), vCC(15)
42	A		1152	1192	1161	1167	1158	42.499	43.251	41.295	63.420	vCC(67), βCH(11)
43	A	1149		1179	1151	1147	1148	5.391	1.794	0.122	0.621	vCC(55), βCH(19)
44	A		1087	1163	1092	1132	1089	0.129	0.778	0.943	1.185	vCC(57), βCH(18)
45	A	1064		1162	1078	1127	1065	18.049	0.148	2.064	3.007	vCN(38), CH ₃ opr(27)
46	A		1044	1125	1061	1099	1058	8.344	7.871	0.421	1.455	vCN(33), vCC(23)
47	A	1028		1094	1039	1076	1028	24.062	31.355	0.334	0.716	CH ₃ ipr(72)
48	A		1001	1068	1013	1050	1004	3.597	4.817	11.980	9.707	CH ₃ opr(60), CH ₃ ops(18)
49	A	989		1043	992	1018	989	6.799	4.954	2.824	1.321	CH ₃ ipr(66)
50	A	958		1039	968	1015	955	1.795	0.968	8.345	10.883	vRing 1(67)
51	A		935	1034	947	1014	934	0.305	0.632	5.942	24.803	vRing 2(69)
52	A	926		1018	931	997	928	0.795	4.760	0.576	0.684	γCH(69), CH ₃ ipr(19)
53	A		913	1015	920	996	917	7.680	0.234	0.197	1.184	CH ₃ opr(37), βRing 1(24)
54	A	904		1001	913	978	902	1.036	3.339	0.451	0.643	γCH(76), CH ₃ ipr(13)
55	A	851	848	980	863	969	850	11.074	3.425	3.501	0.909	γCH(69), vCC(12)
56	A	840		970	845	960	842	15.669	5.971	1.925	4.411	γCH(66), vCC(22)
57	A	830		951	830	938	832	56.830	67.260	2.889	4.071	vCN(42), Ring (20)
58	A	798	794	890	801	870	797	2.851	3.391	3.033	5.637	γCH(80), γCC(13)
59	A		772	872	778	851	779	20.161	43.927	0.671	1.170	γCH(61)
60	A			842	760	819	759	3.078	4.566	3.255	5.219	γCH(69)
61	A			832	758	814	755	12.445	15.490	1.943	2.583	γCH(72), vCC(16)
62	A	746		787	745	779	742	8.451	12.169	26.551	46.526	vCC(70), βCO(14)
63	A	734	739	775	740	763	737	17.288	27.486	0.742	0.467	γCN(43), γCC(20)
64	A		707	732	712	717	705	42.682	52.299	3.908	6.240	γCH(71), vCC(14)
65	A	692		715	704	705	698	4.564	6.719	0.708	1.172	βRing1(54), γCH(12)
66	A	680	685	698	685	696	685	25.959	28.761	0.835	1.086	γRing2(34), βCH(28)
67	A	638		668	639	665	636	1.191	1.317	4.282	6.142	βRing1(59), γCH(24)
68	A	617		651	623	629	620	1.037	0.790	3.714	5.311	βCO(84)
69	A	597	598	619	598	607	598	27.816	26.829	4.756	6.836	βRing2(40), βCC(21)
70	A		565	598	566	568	563	0.638	0.977	12.659	21.354	βCN(39), γCC(27)
71	A	501		533	505	523	504	5.071	3.579	0.872	2.711	βRing1(45), βRing2(16)
72	A		479	512	480	491	480	7.076	6.030	4.454	6.893	γRing1(49), βCC(12)
73	A		426	477	426	468	423	1.156	0.993	3.282	3.826	γRing1(46), γRing2(17)
74	A		416	449	421	430	418	0.471	0.444	5.696	9.556	γRing2(40), βRing(22)
75	A			431	391	421	384	3.761	3.601	6.140	8.823	γCN(39), βCC(21)
76	A			426	369	416	366	0.453	0.631	1.228	2.112	γCN(51), βCC(18)
77	A			377	338	371	335	0.643	1.856	3.083	6.922	γCO(37), τR2(11)
78	A			330	276	314	273	5.594	5.827	6.022	5.372	βCN(37), βCC(24)
79	A			289	261	287	258	2.248	2.477	4.547	9.175	βCN(32), βCC(21)
80	A			250	221	243	218	0.631	0.863	9.354	13.506	βCC(34), CH ₃ ips(31)
81	A			231	209	222	202	0.781	2.244	32.341	39.131	γCC(43), βCC(19)
82	A			207	179	205	176	0.602	0.441	5.151	4.327	βRing1(40), γCC(18)
83	A			180	159	174	156	1.094	1.412	13.893	26.005	βRing2(42), γCC(19)
84	A			166	148	163	145	2.273	4.295	17.541	29.817	βCC(44), γCC(12)
85	A			120	105	104	102	0.650	3.633	61.576	37.169	τCCCO(48), βCO(22)
86	A			102	92	90	89	0.206	0.180	73.885	160.294	γCC(41), βCC(16)
87	A			86	63	69	60	1.061	0.334	65.335	131.192	τCCCO(53), βCC(17)

This reduction occurs because of the electron withdrawal on the carbon atom by the substituent due to the decrease of inductive effect, which in turn is caused by the increased chain length of the substituent [25].

The aromatic C–H in-plane bending vibrations of benzene and its derivatives are observed in the region 1300–1000 cm^{-1} [26]. The bands are sharp but weak to medium intensity. In our present work, the calculated vibrations by DFT methods are predicted at 1267, 1243, 1241, 1183, 1182, 1165 cm^{-1} in B3LYP/6-311+G(d,p) and 1264, 1240, 1238, 1181, 1179 and 1162 cm^{-1} in B3LYP/6-311++G(d,p). These vibrations are assigned to C–H in-plane bending vibration of aromatic ring, and the value B3LYP/6-311++G(d,p) which show good agreement with our experimental values. The out-of-plane bending frequencies of the C–H bands on the aromatic ring are in the region of 950–600 cm^{-1} [27, 28]. The intensities of these vibrations are usually medium or strong. The frequencies of these modes depend mainly on the number of the adjacent hydrogen atoms on the ring and are not significantly affected by the nature of the substituents. Moreover, the substitution patterns on the ring can be judged from the out-of-plane bending of the C–H bands, which appear in the region 900–675 cm^{-1} [28]. In our present study, the C–H out-of-plane bending vibrations are calculated in the region 928–705 cm^{-1} and are well coherence with the experimental data. It can be found that the frequencies increase with decrease of the number of adjacent hydrogen atoms in the benzene ring.

C–C and C=O vibrations

Most of the ring vibrational modes are affected by the substitutions in the ring of the title molecule. The characteristic ring stretching vibrations are assigned in the region 1650–1300 cm^{-1} [29, 30]. Most of the computed frequencies by B3LYP/6-311++G (d,p) method are assigned for C–C and C=C stretching vibrations almost coincides with experimental data. The (C=C) vibrations are more interesting if the double bonds are in conjugation with the ring. The presence of conjugate substituents such as C–O, C–C, C–N or the presence of heavy element causes a doublet formation. Therefore, the C=C stretching vibrations of 4DMBP are found in the range 1628–1319 cm^{-1} in IR and 1609–1315 cm^{-1} in Raman spectrum. The theoretically computed values for C–C vibrational modes by B3LYP/6-311++G (d,p) method give good agreement with experimental data. The calculated C–C–C in-plane bending and out-of-plane bending vibrations are also in good agreement with the experimental data. The ring out-of-plane bending vibrations are calculated at low wavenumbers with maximum PED contribution. The carbon–oxygen double bond is formed by $p_{\pi} - p_{\pi}$ between carbon and oxygen. Because of the different electro negativities of carbon and oxygen atoms, the bonding electrons are not equally distributed between the two atoms. The lone pair of electrons on oxygen also determines the nature of the carbonyl group. The position of the C–O stretching vibration is very sensitive to various factors such as the physical state, electronic effects by substituents, ring strains [31]. Normally carbonyl group vibrations occur in the region 1850–1600 cm^{-1} [32]. In this study, the C–O stretching vibration of 4DMBP is observed at 1636 cm^{-1} in the FT-Raman spectrum, and this mode is confirmed by their PED value of 88%. The calculated frequency is well correlated with the experimental data. The in-plane and out-of-plane bending vibrations of C–O group have also been identified and presented in Table 2.

C–N vibrations

In aromatic compounds, the C–N stretching vibrations usually laid in the region 1400–1200 cm^{-1} . The identification of C–N stretching frequencies was a rather difficult task since the mixing of vibrations was possible in this region [31, 33]. In this study, the bands observed at 1064 cm^{-1} and 1044 cm^{-1} in FT-IR and FT-Raman spectrum had been assigned to C–N stretching vibrations of 4DMBP. The in-plane and out-of-plane bending C–N vibrations had also been identified and presented in Table 2 for the title compound. These assignments were supported by the PED values.

7 Other molecular Properties

7.1 Hyperpolarizability calculations

The first hyperpolarizabilities (β_0) of this novel molecular system, and related properties (β , α_0 and α) of 4DMBP were calculated using B3LYP/6-311+G(d,p) and 6-311++G(d,p) basis set, based on the finite-field approach. In the presence of an applied electric field, the energy of a system is a function of the electric field. Polarizabilities and hyperpolarizabilities characterize the response of a system in an applied electric field [34]. They determine not only the strength of molecular interactions (long-range inter induction, dispersion force, etc.) as well as the cross sections of different scattering and collision process. First hyperpolarizability is a third rank tensor that can be described by $3 \times 3 \times 3$ matrix. The 27 components of the 3D matrix can be reduced to 10 components due to the Kleinman symmetry [35]. It can be given in the lower tetrahedral format. It is obvious that the lower part of the $3 \times 3 \times 3$ matrixes is a tetrahedral. The components of β are defined as the coefficients in the Taylor series expansion of the energy in the external electric field. When the external electric field is weak and homogeneous, this expansion becomes:

$$E = E^0 - \mu_{\alpha} F_{\alpha} - \frac{1}{2} \alpha_{\alpha\beta} F_{\alpha} F_{\beta} - \frac{1}{6} \beta_{\alpha\beta\gamma} F_{\alpha} F_{\beta} F_{\gamma} + \dots$$

where E^0 is the energy of the unperturbed molecules, F_{α} the field at the origin μ_{α} , $\alpha_{\alpha\beta}$ and $\beta_{\alpha\beta\gamma}$ are the components of dipole moments, polarizability and the first hyperpolarizabilities, respectively. The total static dipole moments μ , the mean polarizabilities α_0 , the anisotropy of the polarizabilities α and the mean first hyperpolarizabilities β_0 , using the x, y and z components they are defined as: [36, 37]

The total static dipole moment is

$$\mu = (\mu_x^2 + \mu_y^2 + \mu_z^2)^{1/2}$$

The isotropic polarizability is

$$\alpha_0 = \frac{\alpha_{xx} + \alpha_{yy} + \alpha_{zz}}{3}$$

The polarizability anisotropy invariant is

$$\alpha = 2^{-1/2} [(\alpha_{xx} - \alpha_{yy})^2 + (\alpha_{yy} - \alpha_{zz})^2 + (\alpha_{zz} - \alpha_{xx})^2 + 6\alpha_{xy}^2]^{1/2}$$

and the average hyperpolarizability is

$$\beta_0 = (\beta_x^2 + \beta_y^2 + \beta_z^2)^{1/2}$$

$$\beta_x = \beta_{xxx} + \beta_{yyx} + \beta_{zzx}$$

$$\beta_y = \beta_{yyy} + \beta_{xyy} + \beta_{yyz}$$

$$\beta_z = \beta_{zzz} + \beta_{xxz} + \beta_{yyz}$$

The total static dipole moment, polarizabilities and first hyperpolarizabilities of 4DMBP were calculated. Table 3 lists the values of the electric dipole moment (Debye) and dipole moment components, polarizabilities and hyperpolarizabilities of the 4DMBP. In addition to the isotropic polarizabilities and

polarizabilities anisotropy invariant were also calculated. The polarizabilities and first hyperpolarizabilities of 4DMBP are -91.9453 , -91.3421 a.u and 8.7748×10^{-30} , 9.29297×10^{-30} esu, by B3LYP/6-311+G(d,p) and 6-311++G(d,p) levels, which are comparable with the reported values of similar derivatives [38, 39]. We conclude that the title compound is an attractive object for future studies of nonlinear optical properties.

Table 3. The B3LYP/6-311+G (d,p) and 6-311++G(d,p) calculated electric dipole moments (Debye), Dipole moments compound, polarizability (in a.u), β components and β_{tot} (10^{-30} esu) value of 4-(dimethylamine) benzophenone

Parameters	6-311+G(d,p)	6-311++G(d,p)	Parameters	6-311+G(d,p)	6-311++G(d,p)
μ_x	-3.8871	-4.0656	β_{xxx}	-83.0939	-82.6116
μ_y	-3.4855	-4.0184	β_{yyy}	-20.5366	-28.216
μ_z	0.0169	0.091	β_{zzz}	-0.5991	-0.5654
μ	5.2209	5.717	β_{xyy}	-23.0325	-27.1902
α_{xx}	-72.8561	-70.8652	β_{xxy}	-25.4788	-27.6645
α_{yy}	-101.3699	-101.832	β_{xxz}	-11.5361	-10.6348
α_{zz}	-101.6099	-101.329	β_{zzz}	-2.8689	-2.3196
α_{xy}	-3.8477	-4.844	β_{yyz}	2.7357	2.2477
α	-91.9453	-91.3421	β_{yyz}	4.5405	4.6913
$\Delta\alpha$ (esu)	87.3819×10^{-25}	102.8729×10^{-25}	β_{tot} (esu)	8.7748×10^{-30}	9.29297×10^{-30}

Natural bond orbital analysis

The natural bond orbital (NBO) [14] analysis of 4DMBP are being performed to estimate the delocalization pattern of electron density (ED) between the principal occupied Lewis-type (bond or lone pair) orbitals and unoccupied non-Lewis (antibond or Rydberg) orbitals.

The interactions result is a loss of occupancy from the localized NBO of the idealized Lewis structure into an empty non-Lewis orbital. For each donor (i) and acceptor (j), the stabilization energy $E(2)$ associated with the delocalization from $i \rightarrow j$ is estimated as

$$E(2) = \Delta E_{ij} = q_i \frac{(F_{ij})^2}{(\epsilon_j - \epsilon_i)}$$

Where q_i is the donor orbital occupancy, ϵ_i and ϵ_j are diagonal elements and $F(i,j)$ is the off diagonal NBO Fock matrix element. The NBO analysis provides an efficient method for studying intra and intermolecular bonding and also provides a convenient basis for investigating charge transfer or conjugative interaction in molecular systems [40].

The possibilities of ED delocalization from the lone pair donor atoms to the antibonding acceptor atoms of the title molecule are depicted in Table 4. In other words, the delocalization of ED through donor to the acceptor of this type contributed predominantly to the stabilization of entire molecular system. This is due to the fact that greater the value of $E(2)$, the more intensive is the interaction between electron donors and electron acceptors and the greater the extent of conjugation of the whole system.

The natural charges determined by natural bond orbital (NBO) analysis by B3LYP/6-311+G (d, p) method is presented in the Table 5. The more negative charges on C_4 atoms are due to the attachment of NCH_3 group with these carbon atoms. When compared the charges of the aromatic ring carbon atoms, less negative charge is observed in the carbon atoms which has NCH_3 group. This is due to the hyper conjugative effect of the NCH_3 groups.

The hybrid directionality and bond bending analysis of the benzene ring in the title molecule provide excellent evidence to the substituent effect and steric effect. The angular properties of the natural hybrid orbitals are very much influenced by the type of substituent that causes conjugative effect or steric effect [41]. In Table 5, the bending angles of different bonds are expressed as the angle of deviation from the direction of the line joining two nuclear centers. The $\sigma^*(C_3-C_4)$ bond is more bent away from the line of C_4-C_5 centers by 3.5° results a strong charge transfer path towards NCH_3 group.

Table 4. Significant second-order interaction energy (E (2), kcal/mol) between donor and acceptor orbitals of 4-(dimethylamine) benzophenone calculated at B3LYP/6-311++G(d,p) level of theory

Donor (i)	Acceptor (j)	E(2) ^a kcal/mol	($\epsilon_i - \epsilon_j$) ^b a.u	F_{ij} ^c a.u
σ (C3 - C 4)	σ^* (C3 - H16)	1.54	1.19	0.038
σ (C3 - C 4)	σ^* (C4 - C5)	3.83	1.29	0.063
σ (C3 - C 4)	σ^* (C5 - H26)	2.59	1.18	0.05
σ (C4 - C 5)	σ^* (C3 - C4)	3.98	1.3	0.064
σ (C4 - C 5)	σ^* (C3 - H16)	2.45	1.19	0.048
σ (C4 - N17)	σ^* (C3 - C 4)	1.02	1.3	0.033
σ (C4 - N17)	σ^* (C18 - H20)	1.51	1.19	0.038
σ (C4 - N17)	σ^* (C22 - H24)	1.55	1.19	0.038
σ (N17 - C18)	σ^* (C3 - C4)	1.57	1.28	0.04
σ (N17 - C18)	σ^* (C22 - H23)	1.73	1.17	0.04
σ (N17 - C22)	σ^* (C3 - C4)	1.57	1.28	0.04
σ (N17 - C22)	σ^* (C18 - H21)	1.72	1.17	0.04
σ (C18 - H20)	σ^* (C4 - N17)	3.30	0.88	0.048
σ (C18 - H21)	σ^* (N17 - C22)	3.25	0.86	0.047
σ (C22 - H23)	σ^* (N17 - C18)	3.27	0.85	0.047
σ (C22 - H24)	σ^* (C4 - N17)	3.33	0.88	0.049
π (O14)	π^* (C1 - C7)	1.61	1.09	0.038
π (O14)	π^* (C7 - C13)	1.61	1.09	0.038
π (N17)	π^* (C3 - C4)	1.93	0.88	0.037
π (N17)	π^* (C 4 - C5)	7.63	0.87	0.074
π (N17)	π^* (C18 - H19)	6.58	0.76	0.064
π (N17)	π^* (C22 - H25)	6.67	0.76	0.06

^a E(2) means energy of hyperconjugative interactions.

^b Energy difference between donor and acceptor i and j NBO orbitals.

^c $F(i,j)$ is the Fock matrix element between i and j NBO orbitals

Natural population analysis

The natural population analysis [42] performed on the title molecule clearly describes the distribution of charges in the various sub-shells (core, valence, Rydberg) in the molecular orbital. The accumulation of natural charges on individual atom of the title molecule is given in Table 6. It shows that an atom O_{14} and N_{17} has the most electronegative charge of $-0.5663e$ and $-0.5613e$. Conversely, the H_{16} and H_{26} atoms have considerable electropositive and they are tending to acquire an electron. Further, the natural population analysis showed that 120 electrons in the title molecule are distributed on the sub shell as follows:

Core : 33.98391 (99.9527% of 34)

Valence : 85.67409 (99.6210% of 86)

Rydberg : 0.34200 (0.2850% of 120)

Table 5. Natural atomic orbital occupancies and energies of most interacting NBO's of 4-(dimethylamine) benzophenone along with their hybrid atomic orbitals and hybrid directionality

Parameters ^a (A-B)	Occupancies	Energies (a.u)	Hybrid	AO(%) ^b	Deviation at A(°)	Deviation at B(°)
$\sigma^*(C1-C7)$	0.0642	0.4156	$Sp^{2.44}(C_1)$ $Sp^{1.81}(C_7)$	$s(29.09) + p(70.87)$ $s(35.61) + p(64.34)$	-	-
$\sigma^*(C2-C3)$	0.0175	0.6042	$Sp^{1.83}(C_2)$ $Sp^{1.83}(C_3)$	$s(35.35) + p(64.62)$ $s(35.29) + p(64.68)$	3.8	4.5
$\sigma^*(C3-C4)$	0.0272	0.5990	$sp^{1.80}(C_3)$ $sp^{1.71}(C_4)$	$s(35.67) + p(64.30)$ $s(36.92) + p(63.05)$	4.4	5.2
$\sigma^*(C3-H16)$	0.0146	0.4861	$Sp^{2.46}$	$s(28.93) + p(71.05)$	-	-
$\sigma^*(C4-C5)$	0.0334	0.5911	$sp^{1.75}(C_4)$ $sp^{1.83}(C_5)$	$s(36.40) + p(63.58)$ $s(35.25) + p(64.63)$	3.5	3.3
$\sigma^*(C4-N17)$	0.0353	0.3631	$sp^{2.76}(C_4)$ $sp^{2.56}(N_{17})$	$s(26.56) + p(73.33)$ $s(28.09) + p(71.84)$	2.3	3.2
$\sigma^*(C7-C13)$	0.0645	0.4145	$Sp^{1.81}(C_7)$ $Sp^{2.43}(C_{13})$	$s(35.55) + p(64.40)$ $s(29.11) + p(70.85)$	-	-
$\sigma^*(C7-O14)$	0.0058	0.5753	$Sp^{2.49}(C_7)$ $Sp^{1.29}(O_{14})$	$s(28.62) + p(71.16)$ $s(43.54) + p(56.37)$	-	-
$\sigma^*(N17-C18)$	0.0119	0.3418	$Sp^{2.67}(N_{17})$ $Sp^{3.25}(C_{18})$	$s(27.25) + p(72.68)$ $s(23.50) + p(76.35)$	5.3	2.1
$\sigma^*(N17-C22)$	0.0118	0.3418	$Sp^{2.67}(N_{17})$ $Sp^{3.25}(C_{22})$	$s(27.26) + p(72.67)$ $s(23.50) + p(76.36)$	5.4	2.1
$\sigma^*(C18-H19)$	0.0236	0.4785	$Sp^{2.91}$	$s(25.59) + p(74.38)$	1.2	-
$\sigma^*(C18-H20)$	0.0098	0.4936	$Sp^{2.67}$	$s(25.27) + p(74.70)$	-	-
$\sigma^*(C18-H21)$	0.0059	0.4937	$Sp^{2.67}$	$s(25.60) + p(74.37)$	-	-
$\sigma^*(C22-H23)$	0.0062	0.4941	$Sp^{2.91}$	$s(25.57) + p(74.40)$	-	-
$\sigma^*(C22-H24)$	0.0095	0.4932	$Sp^{2.96}$	$s(25.27) + p(74.70)$	-	-
$\sigma^*(C22-H25)$	0.0236	0.4786	$Sp^{2.90}$	$s(25.62) + p(74.35)$	-	-
$\sigma^*(O14)$	1.9751	-0.6724	$Sp^{0.77}$	$s(56.44) + p(43.54)$	-	-
$\sigma^*(N17)$	1.9071	-0.2833	$Sp^{4.77}$	$s(17.34) + p(82.61)$	-	-

^a For numbering of atoms refer Fig. 1 ^b Percentage of s-type and p-type subshell of an atomic orbitals are given in their respective brackets

Table 6. Accumulation of natural charges and electron population of atoms in core, valance, Rydberg orbitals of 4-(dimethylamine) benzophenone

Atoms ^a	Charge (e)	Natural population (e)			Total (e)	Atoms ^b	Charge (e)	Natural population (e)			Total (e)
		Core	Valence	Rydberg				Core	Valence	Rydberg	
C4	0.1842	1.9988	3.7946	0.0225	5.8158	C1	-0.1442	1.9988	4.1284	0.0170	6.1442
C7	0.5761	1.9991	3.3795	0.0452	5.4239	C2	-0.1428	1.9989	4.1301	0.0139	6.1428
H15	0.1783	0.0000	0.8161	0.0056	0.8217	C3	-0.2189	1.9989	4.2039	0.0162	6.2189
H16	0.2325	0.0000	0.7636	0.0039	0.7675	C5	-0.2418	1.9989	4.2283	0.0146	6.2418
H19	0.1698	0.0000	0.8248	0.0054	0.8302	C6	-0.1669	1.9989	4.1507	0.0172	6.1669
H20	0.2083	0.0000	0.7892	0.0024	0.7917	C8	-0.1774	1.9989	4.1619	0.0166	6.1774
H21	0.2135	0.0000	0.7843	0.0023	0.7865	C9	-0.2141	1.9990	4.2009	0.0142	6.2141
H23	0.2134	0.0000	0.7844	0.0023	0.7867	C10	-0.2007	1.9990	4.1875	0.0142	6.2007
H24	0.2082	0.0000	0.7894	0.0025	0.7918	C11	-0.2150	1.9990	4.2015	0.0144	6.2150
H25	0.1698	0.0000	0.8248	0.0054	0.8303	C12	-0.1517	1.9989	4.1389	0.0139	6.1517
H26	0.2271	0.0000	0.7698	0.0031	0.7729	C13	-0.1380	1.9988	4.1221	0.0171	6.1380
H27	0.2431	0.0000	0.7521	0.0049	0.7569	O14	-0.5663	1.9998	6.5577	0.0089	8.5663
H28	0.2432	0.0000	0.7521	0.0047	0.7568	N17	-0.5613	1.9994	5.5465	0.0153	7.5613
H29	0.2250	0.0000	0.7721	0.0030	0.7750	C18	-0.3876	1.9994	4.3764	0.0119	6.3876
H30	0.2225	0.0000	0.7746	0.0030	0.7776	C22	-0.3870	1.9994	4.3759	0.0118	6.3870
H31	0.2216	0.0000	0.7754	0.0031	0.7784						
H32	0.1772	0.0000	0.8170	0.0058	0.8228						

^b Atoms containing negative charges

^a Atoms containing positive charges

Table 7. Mulliken population analysis of 4-(dimethylamine) benzophenone performed at B3LYP/6-311+G (d,p) and 6-311++G (d,p)

Atoms	Atomic charges		Atom s	Atomic charges	
	B3LYP/6-311+G(d,p)	B3LYP/6-311++G(d,p)		B3LYP/6-311+G(d,p)	B3LYP/6-311++G(d,p)
C1	-0.0373	0.0556	N17	-0.3238	-0.6275
C2	0.0130	-0.1493	C18	0.0850	-0.2336
C3	-0.0198	-0.1663	H19	0.0316	0.1573
C4	0.1869	0.3550	H20	0.0244	0.1462
C5	-0.0164	-0.1569	H21	0.0380	0.1574
C6	0.0689	-0.1485	C22	0.0854	-0.2341
C7	0.1144	0.1795	H23	0.0368	0.1591
C8	0.0613	-0.1253	H24	0.0248	0.1457
C9	0.0388	-0.1354	H25	0.0304	0.1588
C10	0.0375	-0.1120	H26	-0.0360	0.1263
C11	0.0383	-0.1395	H27	-0.0326	0.1607
C12	0.0137	-0.1334	H28	-0.0308	0.1599
C13	-0.0291	0.0445	H29	-0.0266	0.1300
O14	-0.2229	-0.4401	H30	-0.0284	0.1283
H15	-0.0298	0.1424	H31	-0.0288	0.1272
H16	-0.0395	0.1234	H32	-0.0277	0.1447

Electronic absorption spectra

The energies of four important molecular orbitals of 4DMBP the second highest and the highest occupied MO's (HOMO and HOMO-1), the lowest and the second lowest unoccupied MO's (LUMO and LUMO+1) were calculated (Fig. 4). The lowest singlet \rightarrow singlet spin-allowed excited states of 4DMBP were taken into account for the TD-DFT calculation in order to investigate the properties of electronic absorption. The dipole moment in a molecule is another important electronic property that results from non uniform distribution of charges on the various atoms in a molecule. It is mainly used to study the intermolecular interactions involving the van der Waals type dipole-dipole forces, etc., because the larger the dipole moment, stronger will be the intermolecular interactions [43].

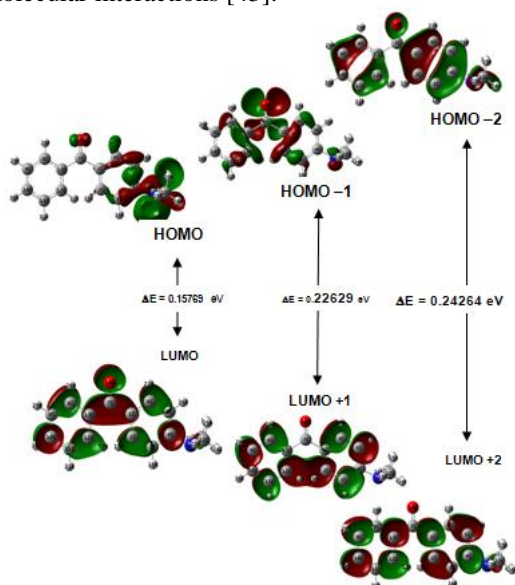


Fig 4. The atomic orbital composition of the frontier molecular orbital for 4-(dimethylamine) benzophenone
Molecular electrostatic potential (MEP) analysis

The molecular electrostatic potential, $V(r)$, at a given point r (x, y, z) in the vicinity of a molecule, is defined in terms of the interaction energy between the electrical charge generated from the molecule electrons and nuclei and a positive test charge (a proton) located at r . The molecular electrostatic potential (MEP) is related to the electronic

density and is a very useful descriptor for determining sites for electrophilic attack and nucleophilic reactions as well as hydrogen-bonding interactions [44, 45]. To predict reactive sites for electrophilic and nucleophilic attack for the title molecule, MEP was calculated at the B3LYP/6-311++G(d,p) optimized geometry. The negative (red) regions of MEP were related to electrophilic reactivity and the positive (white) regions to nucleophilic reactivity shown in Fig.5. The negative regions are mainly localized on the carbonyl oxygen atom, O₁₄ atom. Also, a negative electrostatic potential region is observed around the nitrogen atom (N₁₇ atom). A maximum positive region is localized on the hydrogen atoms indicating a possible site for nucleophilic attack. The MEP map shows that the negative potential sites are on electronegative atoms as well as the positive potential sites are around the hydrogen atoms. These sites give information about the region from where the compound can have noncovalent interactions.

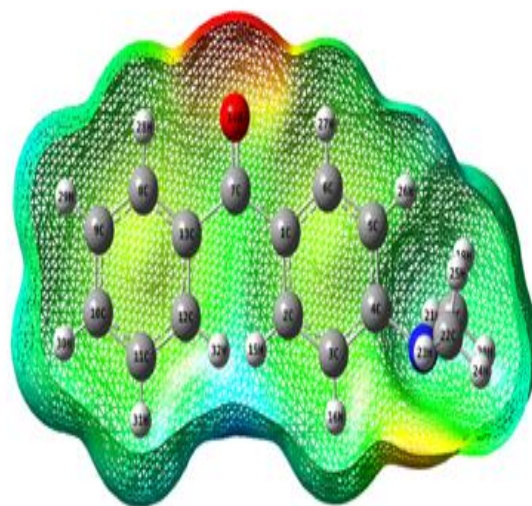


Fig 5. 3D-Molecular electrostatic potential map of 4-(dimethylamine) benzophenone

7.6 Mulliken atomic charge

Mulliken atomic charge calculation has an important role in the application of quantum chemical calculation to molecular system because of atomic charges effect dipole moment, molecular polarizability, electronic structure and more a lot of properties of molecular systems. The calculated Mulliken charge values of 4DMBP are listed in Table 7. The Mulliken charge distribution of the 4DMBP in B3LYP/6-311+G(d,p) and B3LYP/6-311++G(d,p) methods are shown in Fig. 6. The charge distribution of the title molecule shows all the hydrogen atoms and C₄ are positively charged whereas the other carbon atoms are negative. The influence of electronic effect resulting from the hyperconjugation and induction of methylene group in the aromatic ring causes a large positively charged value in the carbon atom C₇ in 4DMBP. The charge changes with basis set presumably occurs due to polarization.

7.7 Thermodynamic function analysis

The total energy of a molecule is the sum of translational, rotational, vibrational and electronic energies. ie, $E = E_t + E_r + E_v + E_e$. The statistical thermo chemical analysis of 4DMBP is carried out considering the molecule to be at room temperature of 298.15 K and one atmospheric pressure. The title molecule is considered as an asymmetric top having rotational symmetry number 1 and the total thermal energy has been arrived as the sum of electronic, translational, rotational and vibrational energies. The variations in the zero point

vibrational energy seem to be insignificant. The thermodynamic quantities such as S , C_p , $(H^0-E^0)/T$ and $(G^0-E^0)/T$ for various temperatures is determined using the vibrational wavenumbers and are presented in Table 8. The following equations are used to predict approximately the values of heat capacity, entropy, energies and partition function for other range of temperatures and the correlation graphs of those is shown in Fig. 7.

$$(S) = 55.56 + 0.279 T - 0.00003T^2 (R^2=1)$$

$$(C_p) = 2.418 + 0.226 T - 0.00009T^2 (R^2=999)$$

$$((H^0 - E^0)/T) = -2.017 + 0.144T - 0.00006T^2 (R^2=999)$$

$$((G^0 - E^0)/T) = -57.58 + 0.134 T - 0.00003T^2 (R^2=999)$$

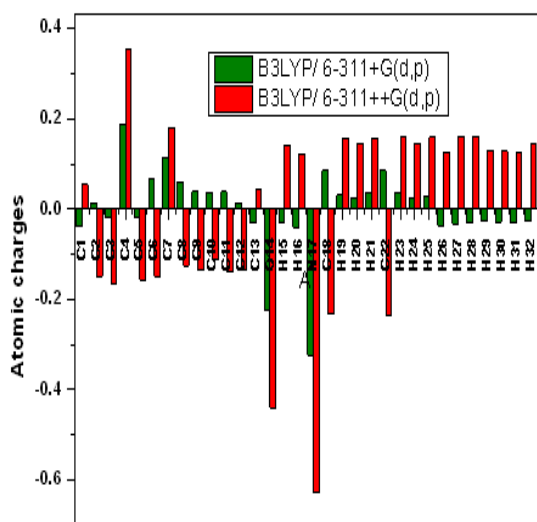


Fig 6. Correlation graph of Mulliken atomic charges with B3LYP/6-311+G(d,p) and B3LYP/6-311++G(d,p) methods
Table 8. Statistical thermodynamic parameters of 4-(dimethylamine) benzophenone at various temperatures

Temp. (Kelvin)	Thermodynamic parameters (k cal mol ^{-N})			
	C _p	S	(H ⁰ - E ⁰)/T	(G ⁰ - E ⁰)/T
100	26.2627928	83.93524	14.2646	-69.6706
200	42.4230978	112.7712	28.4721	-84.2991
300	60.6600277	141.8131	45.46776	-96.3453
400	78.8141292	171.614	64.18316	-107.431
500	94.6243159	202.224	84.20605	-118.018
600	107.641904	233.5342	105.307	-128.227
700	118.274434	265.401	127.3191	-138.082
800	127.044795	297.6903	150.1051	-147.585
900	134.370072	330.2907	173.5488	-156.742
1000	140.551382	363.1133	197.5526	-165.561

Conclusion

The FT-IR and FT-Raman spectral measurements have been made for the 4DMBP. The complete vibrational analysis and first order hyperpolarizability, NBO analysis, HOMO and LUMO analysis, thermodynamic properties of the title compound was performed on the basis of DFT calculations at the B3LYP/6-311+G(d,p) and 6-311++G(d,p) basis sets. The consistency between the calculated and experimental FT-IR and FT-Raman data indicates that the B3LYP/ 6-311++G(d,p) basis set can generates reliable geometry and related properties of the title compound. The difference between the observed and scaled wave number values of most of the fundamentals are very small. Thermodynamic properties in the range from 100 to 1000 K are obtained. The gradients S , C_p , $(H^0-E^0)/T$ and $(G^0-E^0)/T$ to the temperature increases, but that of G decreases, as the temperature increases.

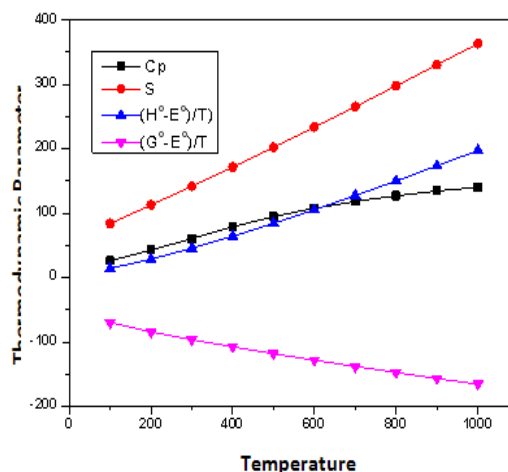


Fig 7. Correlation graph of Gibb's energy, entropy and enthalpy with temperature of 4-(dimethylamine) benzophenone

References

- 1) S. Giorgianni, A. Passerini, A. Gambia, S. Ghersetti, G. Spunta, Spectrosc. Lett. 13 (1980) 445.
- 2) V. Volovsek, G. Baranovic, L. Colombo, J.R. Durig, J. Raman Spectrosc. 22 (1991) 35.
- 3) V. Volovsek, G. Baranovic, L. Colombo, J. Mol. Struct. 266 (1992) 217.
- 4) W. Sasiadek, M. Maczka, E. Kucharska, J. Hanuza, A.A. Kaminskii, H. Klapper, J. Raman Spectrosc. 36 (2005) 912.
- 5) W. Sasiadek, E. Kucharska, J. Hanuza, M. Maczka, A.A. Kaminskii, H. Klapper, Vib. Spectrosc. 43 (2007) 165.
- 6) Gaussian 09, Revision A.1, M.J. Frisch, G.W. Trucks, H.B. Schlegel, G.E. Scuseria, M.A. Robb, J.R. Cheeseman, G. Scalmani, V. Barone, B. Mennucci, G.A. Petersson, H. Nakatsuji, M. Caricato, X. Li, H.P. Hratchian, A.F. Izmaylov, J. Bloino, G. Zheng, J.L. Sonnenberg, M. Hada, M. Ehara, K. Toyota, R. Fukuda, J. Hasegawa, M. Ishida, T. Nakajima, Y. Honda, O. Kitao, H. Nakai, T. Vreven, J. A. Montgomery, Jr., J.E. Peralta, F. Ogliaro, M. Bearpark, J.J. Heyd, E. Brothers, K.N. Kudin, V.N. Staroverov, R. Kobayashi, J. Normand, K. Raghavachari, A. Rendell, J.C. Burant, S.S. Iyengar, J. Tomasi, M. Cossi, N. Rega, J.M. Millam, M. Klene, J.E. Knox, J.B. Cross, V. Bakken, C. Adamo, J. Jaramillo, R. Gomperts, R.E. Stratmann, O. Yazyev, A.J. Austin, R. Cammi, C. Pomelli, J.W. Ochterski, R.L. Martin, K. Morokuma, V.G. Zakrzewski, G.A. Voth, P. Salvador, J.J. Dannenberg, S. Dapprich, A.D. Daniels, Ö. Farkas, J.B. Foresman, J.V. Ortiz, J. Cioslowski, and D.J. Fox, Gaussian, Inc., Wallingford CT, 2009.
- 7) C. Lee, W. Yang, R.G. Parr, Phys. Rev. B37 (1988) 785.
- 8) A.D. Becke, J. Chem. Phys. 98 (1993) 5648.
- 9) A.E. Reed, F. Weinhold, J. Chem. Phys. 83 (1985) 1736.
- 10) H. Lampert, W. Mikenda, A. Karpten, J. Phys. Chem. 101 (1997) 2254.
- 11) G. Fogarasi, X. Zhou, P.W. Taylor and P. Pulay: The Calculation of Ab initio Molecular Geometries: Efficient Optimization by Natural Internal Coordinated and Empirical Correlation by Offset Forces, J. Am. Chem. Soc. 114 (1992) 8191.
- 12) T. Sundius, J. Mol. Struct. 218 (1990) 321: MOLVIBV.7.0; A Program for Harmonic Force Fields calculations, QCPE Program No.807, (2002).
- 13) P.L. Polavarapu, J. Phys. Chem. 94 (1990) 8106.

- 14)G. Keresztury, S. Holly, J. Varga, G. Besenyei, A.V. Wang, J.R. Durig, *Spectrochim. Acta* 49 (1993) 2007.
- 15)M. Tsonkov Kolev, A. Bistra Stamboliyska, *Spectrochim. Acta* 56 (1999) 119.
- 16)R. Dennington II, T. Keith, J. Millam, Gauss View, Version 4. 1. 2, Semichem, Inc. Shawnee Mission, KS, 2007.
- 17)M.D. Halls, J. Velkovski, H.B. Schlegel, *Theor. Chem. Acc.* 105 (2001) 413.
- 18)N.B. Colthup, L.H. Daly, S.E. Wiberley, *Introduction to Infrared and Raman Spectroscopy*, Academic Press, New York, 1964.
- 19)G. Varsanyi, *Vibrational Spectra of Benzene Derivatives*, Academic Press, New York, 1969.
- 20)G. Socrates, *Infrared Characteristics Group Frequencies*, John Wiley, New York 1980
- 21)F.R. Dollish, W.G. Fateley, F.F. Bentley, *Characteristic Raman Frequencies of Organic Compounds*, Wiley, New York, 1997.
- 22)D.N. Singh, I.D. Singh, R.A. Yadav, *Indian J. Phys.* 76 (3) (2002) 307.
- 23)J.H.S. Green, D.J. Harrison, W. Kynoston, *Spectrochim. Acta* 27 (1971) 807.
- 24)J. Coates, in: R.A. Meyers (Edn.), *Interpretation of Infrared Spectra: A Practical Approach*, John Wiley and Sons Ltd., Chichester, 2000.
- 25)H. Spedding, D.H. Whiffen, *Proc. Roy. Soc. London, A* 238 (1956) 245.
- 26)M. Silverstein, G.C. Basseler, C. Morill, *Spectrometric Identification of Organic Compounds*, Wiley, New York, 1981.
- 27)I.F. Shishkov, N.I. Sadova, V.P. Novikov, L.V. Vikov, *Zh. Strukt. Khim.* 25 (1984) 98.
- 28)P.S. Kalsi, *Spectroscopy of Organic Compounds*, Wiley Eastern Ltd., New Delhi, 1993.
- 29)G. Socrates, *Infrared and Raman Characteristic Group Frequencies – Tables and Charts*, Third Edn. Wiley, Chichester, 2001.
- 30)J. Tonannavar, J. Yenagi, V.B. Veenasangeeta Sortur, M.V. Jadhav, Kulkarni, *Spectrochim. Acta* 77 (2010) 351.
- 31)D.N. Sathyanarayana, *Vibrational Spectroscopy - Theory and Applications*, Second Edn., New Age International (P) Ltd. Publishers, New Delhi, 2004.
- 32)R.L. Prasad, A. Kushwaha, M. Suchita, R.A. Kumar, Y. Yadav, *Spectrochim. Acta* 69 (2008) 304.
- 33)M. Karnan, V. Balachandran, M. Murugan, *J. Mol. Struct.* 1039 (2013) 197.
- 34)C.R. Zhang, H.S. Chen, G.H. Wang, *Chem. Res. Chinese. U.* 20 (2004) 640.
- 35)D.A. Kleinman, *Phys. Rev.* 126 (1962) 1977.
- 36)Y. Sun, X. Chen, L. Sun, X. Guo, W. Lu, *J. Chem. Phys. Lett.* 381 (2003) 397.
- 37)O. Christiansen, J. Gauss, J.F. Stanton, *J. Chem. Phys. Lett.* 305 (1999) 147.
- 38)V.B. Jothy, T. Vijayakumar, V.S. Jayakumar, K. Udayalekshmi, K. Ramamoorthy, I. Hubert Joe, *J. Raman Spectrosc.* 38 (2007) 1148.
- 39)O. Prasad, L. Sinha, N. Kumar, *J. Atom. Mol. Sci.* 1 (2010) 201.
- 40)M. Karabacak, L. Sinha, O. Prasad, Z. Cinar, M. Cinar, *Spectrochim. Acta* 93 (2012) 33.
- 41)Ebrahimi, F. Deyhimi, H. Roohi, *J. Mol. Struct. (Theochem)* 626 (2003) 223.
- 42)E. Reed, R.B. Weinstock, F. Weinhold, *J. Chem. Phys.* 83 (1985) 735.
- 43)D P. Chemica, *Scholar Res. Library.* 2 (2010) 48.
- 44)E. Scrocchio, J. Tomasi, *Adv. Quantum Chem.* (1979) 11.
- 45)N. Okulik, A.H. Jubert, *Internet Electron J. Mol. Des.* (2005) 4.